Current Biology 20, 1408–1414, August 10, 2010 ©2010 Elsevier Ltd All rights reserved DOI 10.1016/j.cub.2010.06.024

Report

ASPP2 Regulates Epithelial Cell Polarity through the PAR Complex

Weili Cong,[1,3] Tomonori Hirose,[1,3] Yutaka Harita,[1] Akio Yamashita,[1] Keiko Mizuno,[1] Hisashi Hirano,[2] and Shigeo Ohno[1,*]

[1]Department of Molecular Biology, Yokohama City University Graduate School of Medical Science, 3-9 Fuku-ura, Kanazawa-ku, Yokohama 236-0004, Japan

[2]Supramolecular Biology, International Graduate School of Arts and Sciences, Yokohama City University, 1-7-29 Suehirocho, Tsurumi-ku, Yokohama 236-0045, Japan

Summary

The PAR complex, consisting of the evolutionarily conserved PAR-3, PAR-6, and aPKC, regulates cell polarity in many cell types, including epithelial cells [1–4]. Consistently, genetic manipulation of its components affects tissue integrity in multiple biological systems [5–9]. However, the regulatory mechanisms of the PAR complex remain obscure. We report here that apoptosis-stimulating protein of p53 (ASPP2 or TP53BP2), which binds to the tumor suppressor p53 and stimulates its proapoptotic function [10–12], positively regulates epithelial cell polarity by associating with the PAR complex. ASPP2 interacts and colocalizes with PAR-3 at apical cell-cell junctions in the polarized epithelial cells. Depletion of ASPP2 in epithelial cells causes defects in cell polarity, such as the formation of tight junctions and the maintenance and development of apical membrane domains. Moreover, depletion of ASPP2 causes a defect in PAR-3 localization, as well as vice versa. Furthermore, disturbance in the interaction between ASPP2 and PAR-3 causes defects in cell polarity. We conclude that ASPP2 regulates epithelial cell polarity in cooperation with PAR-3 to form an active PAR complex. Our results, taken together with the known functions of ASPP2, suggest a close relationship between cell polarity and other cell regulatory mechanisms mediated by ASPP2.

Results and Discussion

Apoptosis-Stimulating Protein of p53 Physically Associates with the PAR Complex

Almost all cells are polarized. Typical examples include epithelial cells that show apicobasal polarity, neurons, and directionally migrating cells [3, 4]. Cell polarity is also essential for the asymmetric cell division required for the self-renewal of stem and/or progenitor cells [13, 14]. Another example indicating the importance of cell polarity is the epithelial-mesenchymal transition, a step frequently seen in normal development and in malignant transformation, which involves loss of cell-cell adhesion and cell polarity [15, 16]. Thus, cell polarity is one of the fundamental properties of cells, implicated not only in the normal functioning of tissues but also in many steps of tissue morphogenesis and malignant transformation. However, the relationship between the mechanisms regulating cell polarity and other fundamental cell functions, especially those that determine cell fate, such as growth and survival, mostly remain to be clarified.

In mammalian epithelial cells, the PAR complex plays a central role in the formation of tight junctions (TJs) and the development of apical membrane domains in a process that initiates epithelial polarization [3, 4, 17]. The formation of the PAR complex is induced by the activation of Cdc42 and the recruitment of PAR-3 to the primordial cell-cell contacts [18, 19]. On the other hand, Lgl suppresses the formation of the PAR complex by competing with PAR-3 for interaction with the aPKC-PAR-6 complex [20]. To clarify the regulatory mechanisms of PAR complex formation, we searched for novel proteins interacting with PAR-3. We employed stable lines of epithelial Madin-Darby canine kidney (MDCK) cells in which endogenous PAR-3 was replaced by streptavidin-binding peptide (SBP)-tagged PAR-3, and its expression was controlled by doxycycline to the endogenous level (data not shown). We analyzed the proteins specifically copurified with SBP-tagged PAR-3 and sPAR-3, a short isoform of PAR-3 [21] (see Figure S1A available online). The identified proteins included the previously reported PAR-3-binding proteins, such as atypical protein kinase Cλ (aPKCλ), PAR-6γ, and 14-3-3η. Furthermore, we identified apoptosis-stimulating protein of p53 (ASPP2) as a novel PAR-3-specific binding protein. The specific association between PAR-3 and ASPP2 was verified by cotransfection experiments in 293T cells (Figure 1A).

ASPP2 has been identified as a binding partner of p53 that mediates the apoptotic function of p53 by specifically stimulating the expression of proapoptotic target genes [10–12]. However, the cellular role of ASPP2 in regulating epithelial cell polarity remains to be clarified. We first raised, and confirmed the specificity of, two anti-ASPP2 antibodies, C2 and C3, from different rabbits (Figure S1B). Immunoprecipitation experiments using the C2 antibody revealed an endogenous interaction between PAR-3 and ASPP2 in MDCK cells, supporting the physiological importance of this interaction (Figure 1B). ASPP2 immunoprecipitates also contained aPKCλ and PAR-6β (Figure 1B; see below). However, cotransfection experiments in 293T cells demonstrated a significant interaction of ASPP2 with PAR-3, but not with aPKCλ or PAR-6β (Figure S2A). We found that the N-terminal region of ASPP2 binds to the N- and C-terminal regions of PAR-3 (Figures S2B–S2E). These results suggest that ASPP2 is a novel component of the PAR complex associating via PAR-3. Because the amounts of aPKCλ coprecipitated with PAR-3 or ASPP2 were comparable (Figure 1B), and because Lgl2 did not coprecipitate with ASPP2 (see below), we assume that ASPP2 may preferentially interact with PAR-3, which is associating with aPKC; namely, ASPP2 may preferentially interact with active PAR complexes [22].

ASPP2 Colocalizes with PAR-3 at Apical Cell-Cell Junctions in Epithelial Cells and Tissues

One of the most important properties of the PAR complex is its concentration at the apical cell-cell junctions in polarized

*Correspondence: ohnos@med.yokohama-cu.ac.jp

[3]These authors contributed equally to this work

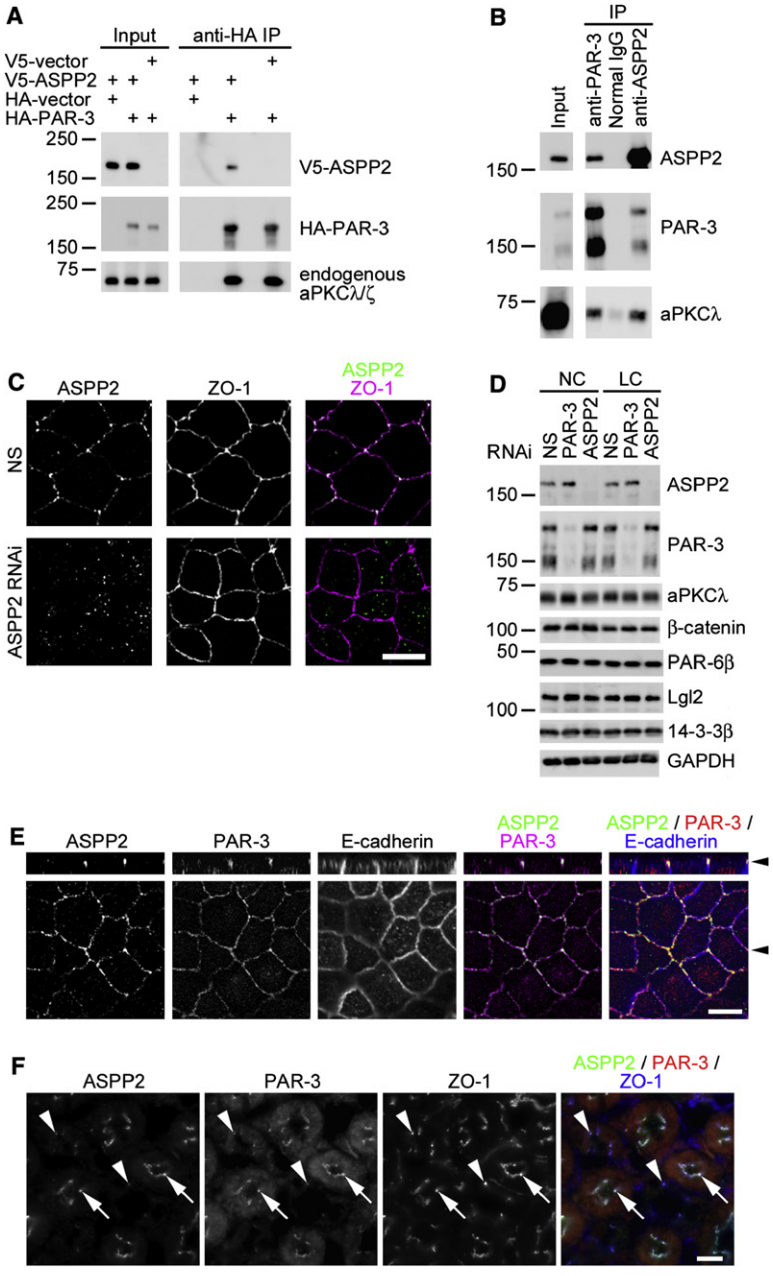

Figure 1. Protein Complex Formation and Colocalization of ASPP2 with PAR-3 and aPKC

(A) 293T cells were transfected with the expression vectors as indicated, and the cell lysates were subjected to immunoprecipitation with anti-HA tag antibody. The cell lysates (input, 0.2%) and coprecipitated proteins (IP, 50%) were analyzed by western blot with anti-V5 tag, anti-HA tag, or anti-aPKCζ/λ antibody.

(B) Madin-Darby canine kidney (MDCK) cells were subjected to immunoprecipitation with anti-ASPP2 C2 antibody, anti-PAR-3 antibody, or normal rabbit IgG as a control. Fractions of cell lysates (input, 1%) and coprecipitated proteins (IP, 25%) were analyzed by anti-ASPP2 C3, anti-PAR-3, or anti-aPKCλ/ι antibody.

(C) Nonsilencing control (NS) or *ASPP2*-knockdown (*ASPP2*-RNAi) stable MDCK clones were cultured on permeable filters for 48 hr and coimmunostained for ASPP2 (C2; green) and ZO-1 (magenta). The panels show representative single confocal sections at the apical side.

(D) Western blot analysis of NS, *PAR-3*-RNAi, and *ASPP2*-RNAi MDCK cells with antibodies against the indicated proteins in both normal (NC) and low (LC) calcium culture conditions. In either condition, the expression of PAR-3 or ASPP2 was specifically reduced in *PAR-3*-RNAi or *ASPP2*-RNAi MDCK cells, respectively. However, the expression of other proteins was not markedly affected.

(E) Confluent MDCK cells on permeable filters were coimmunostained for ASPP2 (C2; green), PAR-3 (magenta or red), and E-cadherin (blue). The upper panels show corresponding z sections of the lower panels, which show single confocal x-y sections at the apical side. Arrowheads indicate the positions of the corresponding x-y or z confocal sections.

(F) Arrows indicate the colocalization of ASPP2 (green), PAR-3 (red), and ZO-1 (blue) to apical cell-cell junctions in columnar epithelial cells in mouse renal tubules. Arrowheads indicate cell-cell junctions with higher ZO-1 signals than ASPP2 or PAR-3 signals.

Scale bars represent 10 μm (C, E, and F).

epithelial cells [2]. To evaluate the physiological relevance of the interaction between ASPP2 and PAR-3, we examined the cellular distribution of ASPP2, because the possible extranuclear functions of mammalian ASPP2 have not been investigated, and its cellular distribution has not been determined. Confocal microscopy using the two anti-ASPP2 antibodies, C2 and C3, in MDCK cells demonstrated a reproducible continuous linear signal in the apical region of the cell-cell contacts (Figure 1C; Figure S3A). Importantly, these signals were diminished by RNA interference (RNAi) for ASPP2, whereas the expression levels of other proteins, including PAR-3, were maintained (Figures 1C and 1D; Figure S3A). In addition, exogenously expressed ASPP2 distributed to the apical region of the cell-cell contacts (Figure S3C). Furthermore, ASPP2 selectively colocalized with PAR-3 and the TJ protein zonula occludens 1 (ZO-1), whereas it was distributed in a mutually exclusive manner with the lateral junction protein E-cadherin (Figures 1C and 1E). These observations strongly support the notion that ASPP2 colocalizes with PAR-3 to apical cell-cell junctions in polarized MDCK cells. 293T cells also demonstrated the colocalization of ASPP2 and PAR-3 at the cell-cell contact sites (Figure S3D).

The characteristic distribution of ASPP2 at apical cell-cell junctions was also observed in highly polarized columnar epithelial cells in mouse tissues such as renal tubules and the small intestine (Figure 1F; Figure S3E). The specificity of this staining was confirmed by preabsorption of anti-ASPP2 antibody with the corresponding antigen. Interestingly, the apical cell-cell junctions of renal epithelial cells showed a variable concentration of ASPP2 and PAR-3 along the nephron. Some of these cells showed a similar variation in the concentration of ASPP2 and PAR-3, whereas that of ZO-1 was virtually constant, suggesting a close relationship between the two proteins (Figure 1F). These results confirm the colocalization of ASPP2 and PAR-3 in polarized epithelial cells in vivo.

ASPP2 Is Involved in the Formation of Tight Junctions

The physical interaction and colocalization between ASPP2 and PAR-3 imply a close functional relationship. Thus, we investigated whether ASPP2 is involved in the cell polarization process, as reported for PAR-3, such as in the formation of TJs and the development of the apical membrane domains [23, 24].

First, we examined the role of ASPP2 in TJ formation. Depolarized control or *ASPP2*-RNAi cells were supplied with calcium (calcium switch, CS) to make cell-cell contacts, and TJ formation was monitored by staining of the TJ proteins ZO-1 and occludin. Although the formation of TJs was accomplished within 6 hr in control cells, *ASPP2*-RNAi cells exhibited a profound delay (Figure 2A). Twenty-four hours after CS, however, there were no apparent differences between control and *ASPP2*-RNAi cells. These properties of *ASPP2*-RNAi cells are very similar to those of *PAR-3*-RNAi cells [23] and suggest the involvement of ASPP2 in the formation of TJs. This notion was further confirmed by a functional measure of TJ integrity, transepithelial electrical resistance (TER) (Figure 2B) [25]. In control cells subjected to CS, the TER rose to a peak 6–8 hr after CS as the junctions matured, followed by a gradual decline. Such development of the TER was significantly abolished in *PAR-3*-RNAi cells, as reported previously [23], and in *ASPP2*-RNAi cells to a lesser extent. Taken together, these results indicate that ASPP2 is involved in the formation of TJs.

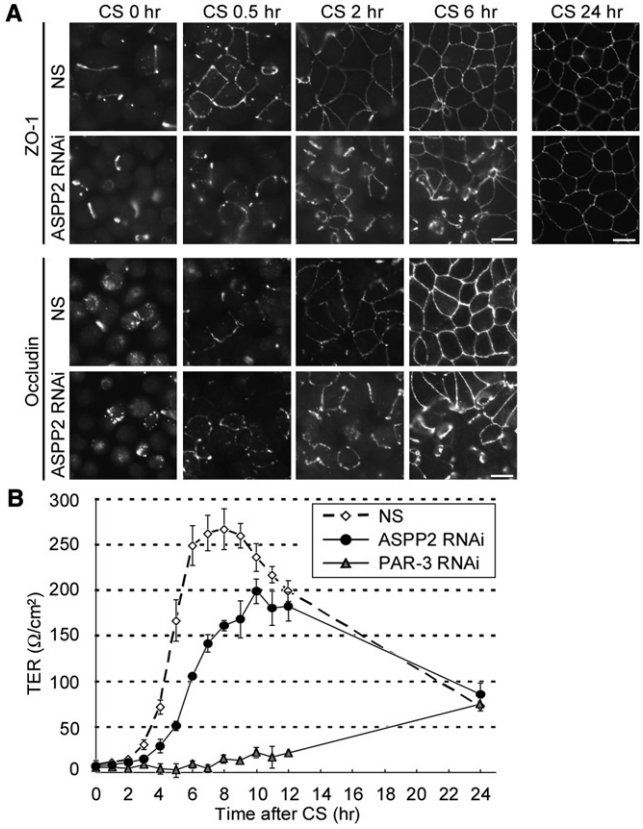

Figure 2. ASPP2 Is Required for the Efficient Formation of Tight Junctions

(A) The time course of tight junction (TJ) formation after calcium switch (CS) was compared between NS and *ASPP2*-RNAi MDCK cells by immunostaining for ZO-1 or occludin. Confluent MDCK cells cultured on permeable filters were subjected to low calcium medium for 20 hr and observed at each time point (0 to 24 hr) after the restoration of calcium, as indicated. Scale bars represent 10 μm.

(B) The development of transepithelial electrical resistance (TER) was compared between NS, *ASPP2*-RNAi, and *PAR-3*-RNAi MDCK cells by measuring it at different times after CS. The error bars indicate the standard deviation (SD; n = 3).

ASPP2 Is Involved in the Development and Maintenance of Apical Domains

We next examined whether ASPP2 plays a role in the development of apical membrane domains, as has been reported for PAR-3 [24]. The formation of apical domains can be monitored by the disappearance of the vacuolar apical compartments (VACs) after CS. VACs represent endocytosed apical membrane proteins that become apparent during depolarization by calcium depletion and are exocytosed to reform apical domains after CS [26]. In control MDCK cells, gp135-positive VACs induced by prolonged calcium depletion were observed in 37% (319 of 859) of cells. CS quickly resulted in the relocalization of gp135 from VACs to apical domains within 3 hr, resulting in 9.5% (115 of 1205) of cells retaining VACs (Figures 3A and 3B), as reported previously [24]. In *ASPP2*-RNAi cells, calcium depletion induced VACs at a similar level (40.9%, 409 of 1000 cells) to that of the control cells. However, the relocalization of gp135 from VACs to apical domains after CS was substantially delayed, with 24.3% (344 of 1418) of cells still containing VACs after 3 hr (Figures 3A and 3B). These effects of *ASPP2*-RNAi were further confirmed by transient transfection with two independent small interfering RNAs (siRNAs) (Figures S4A and S4B). These results indicate that ASPP2 is required for the development of apical domains.

Another measure of epithelial cell polarity mediated by the PAR complex is the recruitment of apical proteins to the cell surface from the intracellular compartment during the maintenance phase of cell polarity [22]. This phenomenon was clearly demonstrated in MDCK cells in the absence of cell-cell contact induced by low calcium conditions. Many control cells retained apical proteins such as gp135 at the cell periphery (nonsilencing, NS; Figure 3C). This apical domain retention was significantly affected in *PAR-3*-RNAi cells [22] (Figure 3D). Similarly, but to a lesser extent, *ASPP2*-RNAi cells failed to retain apical domain proteins; gp135, ezrin, and F-actin failed to distribute to the cell periphery and instead accumulated in the intracellular regions (Figure 3C). The proportion of cells retaining gp135 at the cell periphery was significantly lower in *ASPP2*-RNAi cells (28% ± 6%, n = 3) than in control cells (67% ± 2%, n = 3) (Figure 3D). Consistent results were obtained by transient transfection with two independent siRNAs against *ASPP2* (Figure S4C). These data indicate that ASPP2 is required for the maintenance of apical domains.

ASPP2 Colocalizes with PAR-3 to Primordial Cell-Cell Contacts

Physical interaction and an intimate functional relationship between ASPP2 and PAR-3 suggest the importance of the colocalization of ASPP2 and PAR-3 in the regulation of epithelial cell polarity. We compared the distribution of ASPP2 and PAR-3 during the polarization process. In polarized MDCK cells, ASPP2 and the components of the PAR complex localize to the apical junctions (Figures 1C and 1E) [20, 27]. On the other hand, they move to different compartments in depolarized cells: aPKC and PAR-6β move to VACs, whereas PAR-3 remains at the cell periphery (Figure 3F), although the exact destination of PAR-3 has not been established [24]. Importantly, ASPP2 was not detected in VACs, but it distributed to the cell periphery and to the remaining cell-cell contacts with ZO-1 (Figures 3E and 3F), showing a sharp contrast to aPKC and PAR-6. Note that nonspecific signals were possibly observed following nuclear staining of ASPP2 under low calcium conditions, because only the signals in cell-cell junctions were diminished by RNAi against *ASPP2* (Figure S3B). Furthermore, ASPP2 and PAR-3 colocalized to the fragmentally remaining cell-cell contacts labeled with ZO-1 in low

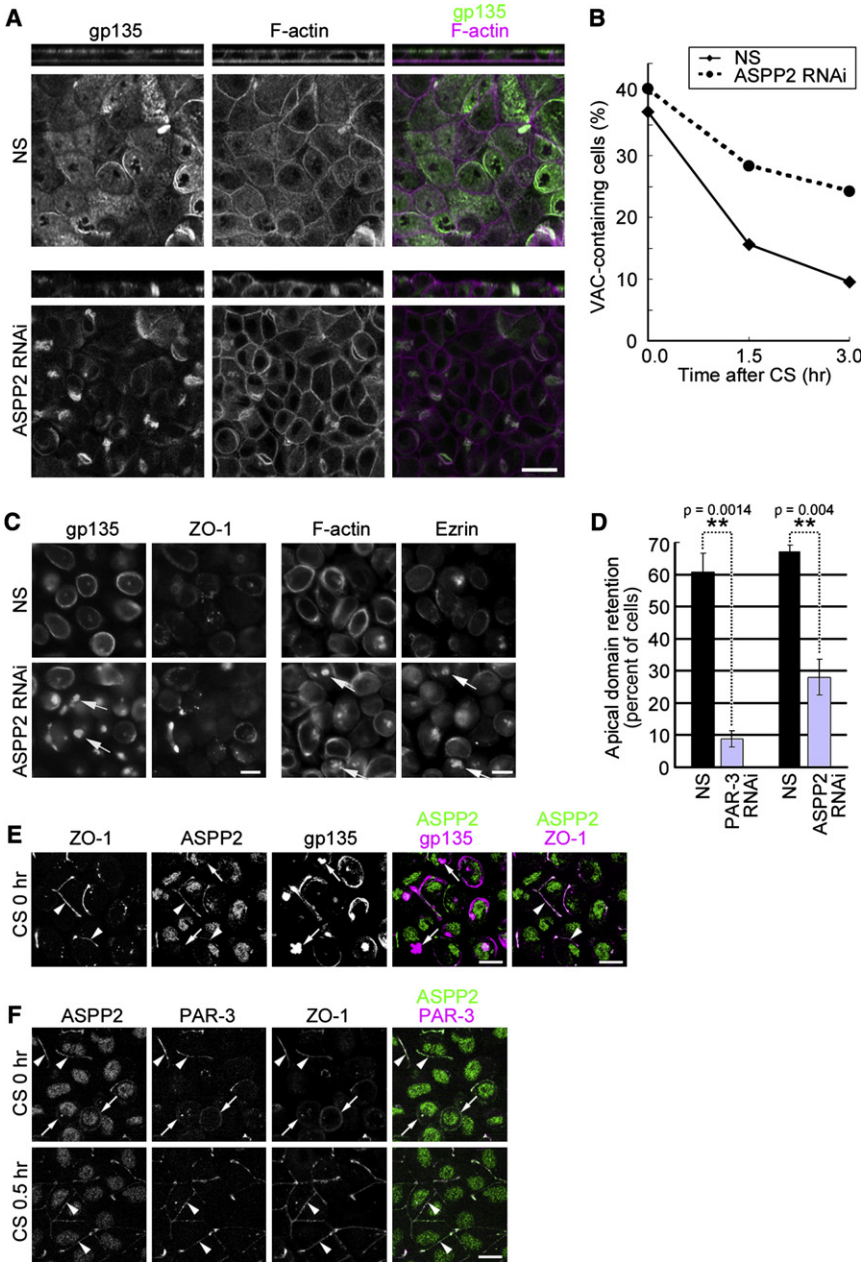

Figure 3. ASPP2 Is Required for the Development and Maintenance of Apical Domains in MDCK Cells

(A) The development of apical domains was assessed 3 hr after CS in NS and *ASPP2*-RNAi MDCK cells. The apical domains were labeled with gp135, and the whole cell cortices, including the vacuolar apical compartments (VACs), were labeled for F-actin. Projected views of confocal sections are presented with z sectional views. *ASPP2*-RNAi cells contain large intracellular aggregates positive for gp135 and F-actin, representing VACs, which indicate failure of appropriate apical domain development.

(B) The time courses of VAC exocytosis induced by CS (time 0) were quantified for NS control (diamonds) and *ASPP2*-RNAi (circles) MDCK cells.

(C) Confluent monolayers of NS and *ASPP2*-RNAi MDCK cells on permeable filters were subjected to low calcium medium for more than 20 hr. The retention of apical domains was analyzed by labeling for gp135, F-actin, or ezrin, whereas the disassembled cell-cell junctions were confirmed by labeling for ZO-1 or F-actin. The representatives from three independent experiments are shown, and each photograph represents the projected views of confocal sections from the apical to the basal membrane of cells. Arrows indicate VACs.

(D) Quantification of the cells retaining apical domains with peripheral gp135 staining, as indicated in (C). *PAR-3*-RNAi cells served as a positive control for the experimental procedures. The percentage of the total cells (at least 460 cells) is shown as the mean value (±SD) of three independent experiments. The p values were determined by two-tailed Student's t test.

(E) Confluent MDCK cells cultured on a permeable filter were subjected to a low calcium medium for 20 hr. VACs are identified as large intracellular structures strongly stained for gp135, a representative marker for apical domains (arrows). ASPP2 colocalizes with ZO-1 at the remaining cell-cell contacts (arrowheads).

(F) MDCK cells cultured for more than 20 hr in low calcium conditions were restored with 1.8 mM Ca^{2+} for 30 min (CS 0.5 hr). The localization of ASPP2 (green), PAR-3 (magenta), and ZO-1 is demonstrated in projected views of optical sections from the apical to the basal membranes of cells. Proteins distributed at the cell periphery and cell-cell contacts are indicated by arrows and arrowheads, respectively.

Scale bars represent 10 μm (A, C, E, and F).

calcium conditions and to the primordial cell-cell contacts during epithelial polarization shortly after restoring calcium (Figure 3F). These observations strongly support the occurrence of the ASPP2-PAR-3 complex at primordial cell-cell contacts before aPKC-PAR-6β is recruited to PAR-3 [24, 28].

ASPP2 Forms a Protein Complex with PAR-3 Independently of Lgl

The activity of the PAR-3-aPKC-PAR-6 complex is negatively regulated by Lgl, which competes for the aPKC-PAR-6 complex with PAR-3 [22]. To evaluate the involvement of ASPP2 in this process, we examined whether Lgl-1/2 affected the interaction between ASPP2 and PAR-3. Depletion of Lgl-1/2 clearly increased the amounts of aPKC and PAR-6β coprecipitated with PAR-3, confirming the enhanced association of the aPKC-PAR6β complex with PAR-3 (Figure 4A) [22]. However, depletion of Lgl-1/2 did not significantly affect the amount of ASPP2 coprecipitated with PAR-3. Consistently, depletion of Lgl-1/2 did not significantly increase the amount of PAR-3 coprecipitated with ASPP2, whereas the levels of aPKC and PAR-6β were increased. These results suggest that the interaction between ASPP2 and PAR-3 is independent of Lgl. Taken together with the colocalization of ASPP2 and PAR-3 from the initial phase of polarization, our observations support the intimate relationship between these proteins.

The Interaction between ASPP2 and PAR-3 Is Required for Epithelial Cell Polarity

The close functional relationship and colocalization of ASPP2 and PAR-3 allowed us to examine the mutual relationship between ASPP2 and PAR-3 in terms of their localization. We found that the signals for ASPP2 in cell-cell junctions were

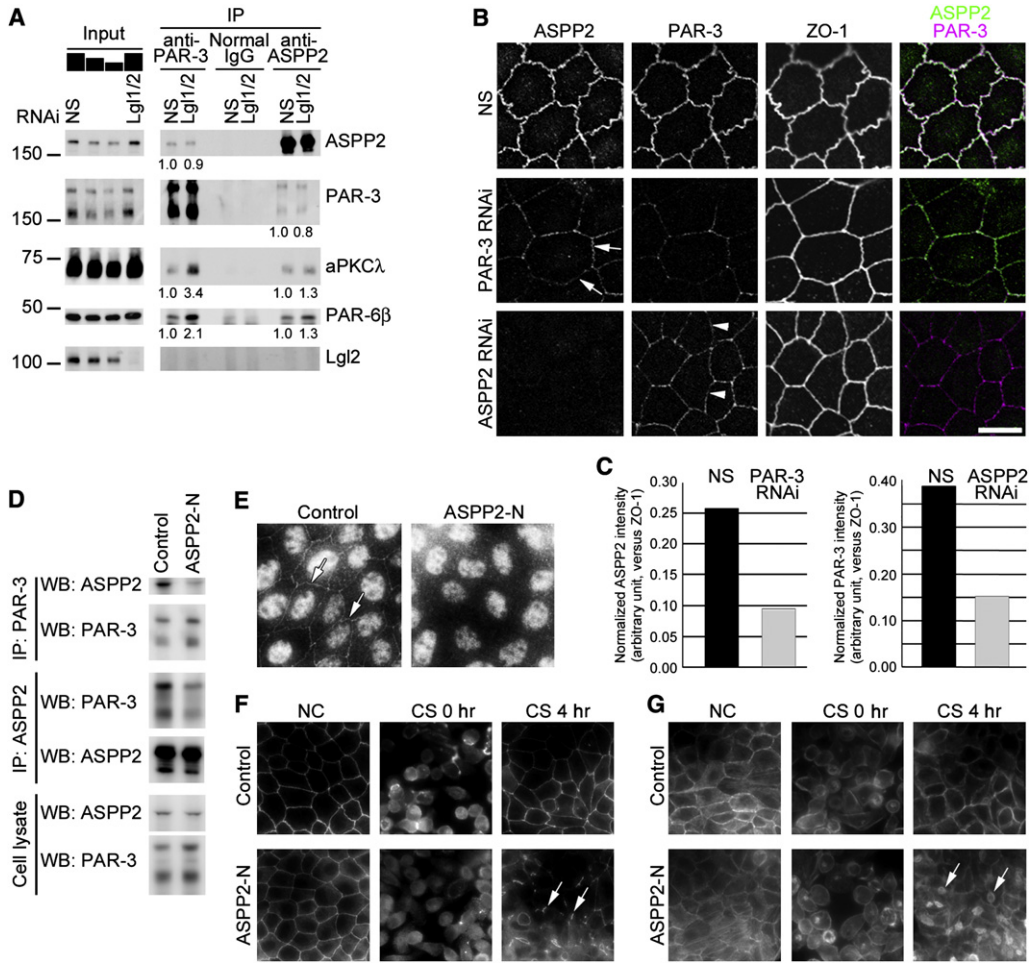

Figure 4. Interaction between ASPP2 and PAR-3 Is Required for Epithelial Cell Polarity

(A) NS and *Lgl-1/2* double RNAi MDCK cells were subjected to immunoprecipitation with the indicated antibodies. Fractions of the cell lysate (input: NS, 0.3%, 0.2%, and 0.15%; *Lgl-1/2*-RNAi, 0.3%) and coprecipitated proteins (IP, 20% each) were analyzed by western blotting using antibodies against the indicated proteins. Relative intensities are shown in numbers below the bands.

(B) ASPP2 (green), PAR-3 (magenta), and ZO-1 were localized in confluent monolayers of NS, *PAR-3*-RNAi, and *ASPP2*-RNAi MDCK cells. Single confocal sections at the apical side demonstrate substantially diminished signals for ASPP2 (arrows) or PAR-3 (arrowheads) in the cell-cell junctions in *PAR-3*- or *ASPP2*-RNAi cells, respectively. Instead, the signals for ZO-1 were not notably altered. Scale bar represents 10 μm.

(C) Quantification of the normalized signals for ASPP2 (top) or PAR-3 (bottom) in *PAR-3*- or *ASPP2*-RNAi cells, respectively. The signals were normalized against ZO-1 staining, and the means of two independent experiments are shown.

(D) MDCK cells expressing or not expressing the N-terminal part of ASPP2 (ASPP2-N) were subjected to immunoprecipitation with the indicated antibodies. Fractions of the cell lysate and coprecipitated proteins were analyzed by western blotting using the indicated antibodies.

(E) The localization of endogenous ASPP2 was analyzed in control and ASPP2-N-expressing MDCK cells. The signals for ASPP2 were substantially reduced in ASPP2-N-expressing MDCK cells (arrows).

(F and G) The formation of TJs and apical domains after CS was compared between control and ASPP2-N-expressing MDCK cells by labeling for ZO-1 (F) or F-actin (G). Arrows indicate incomplete formation of TJs (F) or remaining VACs (G).

substantially diminished in *PAR-3*-RNAi cells, although RNAi against either *ASPP2* or *PAR-3* did not apparently affect the signals for ZO-1 in confluent MDCK cells (Figures 4B and 4C). Similarly, the signals for PAR-3 were significantly reduced in *ASPP2*-RNAi cells. Note that the expression level of ASPP2 was not affected in *PAR-3*-RNAi cells, and vice versa, in either normal or low calcium conditions (Figure 1D). These results indicate the mutual dependence of ASPP2 and PAR-3 for their localization at apical cell-cell junctions, further supporting the close functional relationship between ASPP2 and the PAR complex.

To investigate the physiological significance of the interaction between ASPP2 and PAR-3, we utilized overexpression of the N-terminal part of ASPP2 (ASPP2-N; Figure S2E) to perturb this interaction. Immunoprecipitation analysis of MDCK cells expressing ASPP2-N revealed interference in the formation of the complex between endogenous ASPP2 and PAR-3 (Figure 4D). These cells demonstrated reduced localization of endogenous ASPP2 at cell-cell junctions, suggesting that the localization is dependent on the interaction with PAR-3 (Figure 4E). Importantly, these cells also showed delayed formation of cell-cell junctions and apical domains after CS (Figures 4F and 4G). These data demonstrate that the interaction between ASPP2 and PAR-3 is important in the regulation of epithelial cell polarity.

Conclusions

In this study, we provide evidence that ASPP2 plays critical roles in the establishment and maintenance of epithelial

apical-basal polarity by mediating the PAR complex formation through the regulation of PAR-3 localization. In addition to epithelial polarity, the PAR complex has been shown to regulate asymmetric cell division [1, 13, 14]. Furthermore, a recent report has shown that p53 regulates the polarity of self-renewing division of mammary stem cells [29]. However, the molecular mechanisms have not yet been elucidated. Considering the role of ASPP as an important mediator of p53 [10, 12], our data may shed light on a possible link between cell fate determination by p53 and the regulation of cell polarity by the ASPP2-PAR-3 complex.

Experimental Procedures

Cell Culture

MDCK II cells were grown in Dulbecco's modified Eagle's medium (DMEM; Nissui Pharmaceutical) containing 10% fetal calf serum (FCS), penicillin, and streptomycin (BioWhittaker) at 37°C in a 5% CO_2 atmosphere at constant humidity. For the Ca^{2+}-depletion assay, cells were seeded on Transwell filters (12 mm diameter, 0.4 μm pore size; Corning Coaster) at 2×10^5 cells/cm^2 and grown for 1 or 2 days to produce a confluent monolayer. Cells were washed twice with phosphate-buffered saline and incubated in a low Ca^{2+} (LC) medium containing 5% FCS, 3 μM Ca^{2+}, penicillin, and streptomycin for more than 20 hr. The Ca^{2+} switch assay was performed by replacing the LC medium restored with 1.8 mM Ca^{2+}.

Expression Vectors

For generating MDCK cells stably expressing SBP-tagged proteins under the control of tetracycline-inducible transactivation, the SacI-PvuI fragment of the pNTAP vector (Stratagene) was first cloned into the EcoRV and PstI sites of the pOS-Tet14MCS vector (a generous gift from Y. Miwa, Tsukuba University) after blunting, and then a cDNA encoding rat PAR-3 (1–1333 aa) [27] or mouse sPAR-3 (1–1034 aa) [21] was cloned into the EcoRV site. cDNAs encoding rat PAR-3 (1–1333 aa) and human ASPP2 (2–1128 aa; IMAGE cDNA clone ID 4537206, GenBank ID Q13625) were subcloned into the SR-HA and SR-V5 mammalian expression vectors, respectively.

RNAi for *ASPP2* in MDCK Cells

Nonsilencing control and *ASPP2*-RNAi MDCK clones were established by stable transfection with pSUPERIOR.neo vectors (Oligoengine) encoding a scramble sequence (5′-CAGUCGCGUUUGCGACUGG-3′; Dharmacon Research) [22, 30] and the canine *ASPP2* siRNA sequence (*ASPP2*-siRNA1, #2315: 5′-GCACUUCUCCACUGUUUAUGG-3′), respectively. The *PAR-3*-RNAi MDCK stable clone was described previously [22]. The sequences of siRNAs used were nonsilencing control (QIAGEN Cat# 1027281), *ASPP2*-siRNA1 (#2315), and *ASPP2*-siRNA2 (#3326: 5′-GUUCCUCGUGCAAUUUG GUGU-3′). The *ASPP2* siRNAs were designed to avoid any off-target effects on ASPP1 or iASPP.

Immunoprecipitation and Western Blot Analysis

MDCK II and 293T cells were lysed in lysis buffer containing 50 mM Tris-HCl at pH 7.5, 150 mM NaCl, 10% glycerol, 1% NP-40, 5 mM $MgCl_2$, 1 mM EGTA, 1 mM dithiothreitol, protease inhibitor cocktail (SIGMA), and phosphatase inhibitor cocktail (Roche). After centrifugation at 20,000 × g for 30 min, the supernatants were subjected to immunoprecipitation with the indicated antibodies followed by SDS-PAGE and western blotting, as described previously [22].

Antibodies

The rabbit anti-ASPP2 antibodies, C2AP and C3AP, were raised against aa 773–912 of human ASPP2 fused with glutathione-*S*-transferase and were affinity purified (Scrum). Rat anti-PAR-3 polyclonal antibody (pAb) (CR1-2AP) and rabbit anti-PAR-6β pAb (BC31AP) were described previously [20, 24]. Antibodies purchased were rabbit anti-PAR-3 pAb (07-330; Upstate), mouse anti-aPKCι monoclonal antibody (mAb; clone 23; BD Transduction Laboratories), mouse anti-occludin mAb (clone OC-3F10; Zymed), mouse anti-E-cadherin mAb (clone 36; BD Transduction Laboratories), rabbit anti-aPKCζ/λ pAb (SC-216; Santa Cruz Biotechnology), rat anti-ZO-1 mAb (clone R40.76; Santa Cruz Biotechnology), rabbit anti-14-3-3β pAb (SC-629; Santa Cruz Biotechnology), mouse anti-ezrin mAb (clone 3C12; Sigma), and mouse anti-Lgl2 mAb (clone 4G2; Abnova). Mouse anti-gp135 mAb (clone 3F2/D8) was a gift from George K. Ojakian (State University of New York).

Immunofluorescence Microscopy

MDCK cells were fixed with 2% paraformaldehyde (PFA) and stained as described previously [31]. The primary antibodies were visualized using Alexa Fluor 488-, 555-, or 647-conjugated secondary antibodies (Molecular Probes). Rhodamine-phalloidin was used to visualize filamentous actin (Molecular Probes). Samples were mounted with ProLong Gold (Invitrogen) and were observed using a confocal microscope system (LSM 510; Carl Zeiss) or a fluorescence microscope (BX50; Olympus) equipped with a cooled charge-coupled device camera (Sensys 1400G2; Photometrics). Acquired images were analyzed using Photoshop (Adobe Systems), Multi Gauge (Fujifilm), or ImageJ (National Institutes of Health), according to the guidelines of the journal.

Mouse (ICR; Japan CLEA) kidneys and duodenum were perfused and immersed in 0.1 M HEPES-NaOH buffer (pH 7.4) containing 4% PFA, 2.5 mM $CaCl_2$, 1.25 mM $MgCl_2$, and 2.9% glucose for 2 hr at room temperature [32] and were processed for cryosectioning. The cryosections were processed for heat-induced epitope retrieval by incubating in a target retrieval solution (S1700; DAKO) for 15 min at 121°C, and they were labeled with anti-ASPP2 antibody (2.5 μg/ml, 16.7 nM) with 3.0 nM of the corresponding antigen or GST. All animal experiments were conducted in accordance with the Guidelines for Proper Conduct of Animal Experiments (Science Council of Japan), and all protocols were approved by our institutional review boards.

Supplemental Information

Supplemental Information includes four figures and can be found with this article online at doi:10.1016/j.cub.2010.06.024.

Acknowledgments

We are grateful to Y. Miwa and G.K. Ojakian for reagents, all the members of the Ohno laboratory for helpful discussions, and Rie Kurata and Chiho Kusaka for their technical assistance. This work was supported by the Yokohama City University Center of Excellence Program of the Ministry of Education, Culture, Sports, Science and Technology of Japan (MEXT) (S.O.). This work was also supported in part by grants from the Japan Society for the Promotion of Science and from MEXT (T.H., Y.H., A.Y., K.M., H.H., and S.O.) and by a grant from the 2009 Strategic Research Project of Yokohama City University (T.H.).

Received: December 4, 2009
Revised: May 21, 2010
Accepted: June 10, 2010
Published online: July 8, 2010

References

1. Kemphues, K. (2000). PARsing embryonic polarity. Cell *101*, 345–348.
2. Ohno, S. (2001). Intercellular junctions and cellular polarity: The PAR-aPKC complex, a conserved core cassette playing fundamental roles in cell polarity. Curr. Opin. Cell Biol. *13*, 641–648.
3. Suzuki, A., and Ohno, S. (2006). The PAR-aPKC system: Lessons in polarity. J. Cell Sci. *119*, 979–987.
4. Goldstein, B., and Macara, I.G. (2007). The PAR proteins: Fundamental players in animal cell polarization. Dev. Cell *13*, 609–622.
5. Hirose, T., Karasawa, M., Sugitani, Y., Fujisawa, M., Akimoto, K., Ohno, S., and Noda, T. (2006). PAR3 is essential for cyst-mediated epicardial development by establishing apical cortical domains. Development *133*, 1389–1398.
6. Imai, F., Hirai, S., Akimoto, K., Koyama, H., Miyata, T., Ogawa, M., Noguchi, S., Sasaoka, T., Noda, T., and Ohno, S. (2006). Inactivation of aPKClambda results in the loss of adherens junctions in neuroepithelial cells without affecting neurogenesis in mouse neocortex. Development *133*, 1735–1744.
7. Costa, M.R., Wen, G., Lepier, A., Schroeder, T., and Götz, M. (2008). Par-complex proteins promote proliferative progenitor divisions in the developing mouse cerebral cortex. Development *135*, 11–22.
8. Hirose, T., Satoh, D., Kurihara, H., Kusaka, C., Hirose, H., Akimoto, K., Matsusaka, T., Ichikawa, I., Noda, T., and Ohno, S. (2009). An essential

role of the universal polarity protein, aPKClambda, on the maintenance of podocyte slit diaphragms. PLoS ONE *4*, e4194.

9. Bultje, R.S., Castaneda-Castellanos, D.R., Jan, L.Y., Jan, Y.N., Kriegstein, A.R., and Shi, S.H. (2009). Mammalian Par3 regulates progenitor cell asymmetric division via notch signaling in the developing neocortex. Neuron *63*, 189–202.
10. Trigiante, G., and Lu, X. (2006). ASPP [corrected] and cancer. Nat. Rev. Cancer *6*, 217–226.
11. Vives, V., Su, J., Zhong, S., Ratnayaka, I., Slee, E., Goldin, R., and Lu, X. (2006). ASPP2 is a haploinsufficient tumor suppressor that cooperates with p53 to suppress tumor growth. Genes Dev. *20*, 1262–1267.
12. Sullivan, A., and Lu, X. (2007). ASPP: A new family of oncogenes and tumour suppressor genes. Br. J. Cancer *96*, 196–200.
13. Knoblich, J.A. (2008). Mechanisms of asymmetric stem cell division. Cell *132*, 583–597.
14. Morrison, S.J., and Kimble, J. (2006). Asymmetric and symmetric stem-cell divisions in development and cancer. Nature *441*, 1068–1074.
15. Kalluri, R., and Weinberg, R.A. (2009). The basics of epithelial-mesenchymal transition. J. Clin. Invest. *119*, 1420–1428.
16. Bryant, D.M., and Mostov, K.E. (2008). From cells to organs: Building polarized tissue. Nat. Rev. Mol. Cell Biol. *9*, 887–901.
17. Wang, Q., and Margolis, B. (2007). Apical junctional complexes and cell polarity. Kidney Int. *72*, 1448–1458.
18. Etienne-Manneville, S. (2004). Cdc42—the centre of polarity. J. Cell Sci. *117*, 1291–1300.
19. Iden, S., and Collard, J.G. (2008). Crosstalk between small GTPases and polarity proteins in cell polarization. Nat. Rev. Mol. Cell Biol. *9*, 846–859.
20. Yamanaka, T., Horikoshi, Y., Sugiyama, Y., Ishiyama, C., Suzuki, A., Hirose, T., Iwamatsu, A., Shinohara, A., and Ohno, S. (2003). Mammalian Lgl forms a protein complex with PAR-6 and aPKC independently of PAR-3 to regulate epithelial cell polarity. Curr. Biol. *13*, 734–743.
21. Mizuno, K., Suzuki, A., Hirose, T., Kitamura, K., Kutsuzawa, K., Futaki, M., Amano, Y., and Ohno, S. (2003). Self-association of PAR-3-mediated by the conserved N-terminal domain contributes to the development of epithelial tight junctions. J. Biol. Chem. *278*, 31240–31250.
22. Yamanaka, T., Horikoshi, Y., Izumi, N., Suzuki, A., Mizuno, K., and Ohno, S. (2006). Lgl mediates apical domain disassembly by suppressing the PAR-3-aPKC-PAR-6 complex to orient apical membrane polarity. J. Cell Sci. *119*, 2107–2118.
23. Chen, X., and Macara, I.G. (2005). Par-3 controls tight junction assembly through the Rac exchange factor Tiam1. Nat. Cell Biol. *7*, 262–269.
24. Horikoshi, Y., Suzuki, A., Yamanaka, T., Sasaki, K., Mizuno, K., Sawada, H., Yonemura, S., and Ohno, S. (2009). Interaction between PAR-3 and the aPKC-PAR-6 complex is indispensable for apical domain development of epithelial cells. J. Cell Sci. *122*, 1595–1606.
25. Madara, J.L., and Dharmsathaphorn, K. (1985). Occluding junction structure-function relationships in a cultured epithelial monolayer. J. Cell Biol. *101*, 2124–2133.
26. Vega-Salas, D.E., Salas, P.J., and Rodriguez-Boulan, E. (1988). Exocytosis of vacuolar apical compartment (VAC): A cell-cell contact controlled mechanism for the establishment of the apical plasma membrane domain in epithelial cells. J. Cell Biol. *107*, 1717–1728.
27. Izumi, Y., Hirose, T., Tamai, Y., Hirai, S., Nagashima, Y., Fujimoto, T., Tabuse, Y., Kemphues, K.J., and Ohno, S. (1998). An atypical PKC directly associates and colocalizes at the epithelial tight junction with ASIP, a mammalian homologue of Caenorhabditis elegans polarity protein PAR-3. J. Cell Biol. *143*, 95–106.
28. Suzuki, A., Ishiyama, C., Hashiba, K., Shimizu, M., Ebnet, K., and Ohno, S. (2002). aPKC kinase activity is required for the asymmetric differentiation of the premature junctional complex during epithelial cell polarization. J. Cell Sci. *115*, 3565–3573.
29. Cicalese, A., Bonizzi, G., Pasi, C.E., Faretta, M., Ronzoni, S., Giulini, B., Brisken, C., Minucci, S., Di Fiore, P.P., and Pelicci, P.G. (2009). The tumor suppressor p53 regulates polarity of self-renewing divisions in mammary stem cells. Cell *138*, 1083–1095.
30. Suzuki, A., Hirata, M., Kamimura, K., Maniwa, R., Yamanaka, T., Mizuno, K., Kishikawa, M., Hirose, H., Amano, Y., Izumi, N., et al. (2004). aPKC acts upstream of PAR-1b in both the establishment and maintenance of mammalian epithelial polarity. Curr. Biol. *14*, 1425–1435.
31. Hirose, T., Izumi, Y., Nagashima, Y., Tamai-Nagai, Y., Kurihara, H., Sakai, T., Suzuki, Y., Yamanaka, T., Suzuki, A., Mizuno, K., and Ohno, S. (2002). Involvement of ASIP/PAR-3 in the promotion of epithelial tight junction formation. J. Cell Sci. *115*, 2485–2495.
32. Yamashita, S., Katsumata, O., and Okada, Y. (2009). Establishment of a standardized post-embedding method for immunoelectron microscopy by applying heat-induced antigen retrieval. J. Electron Microsc. (Tokyo) *58*, 267–279.